

# Characterisation and properties of fine-scale PZT fibres

A.C. Dent <sup>\*a</sup>, L.J. Nelson <sup>a</sup>, C.R. Bowen <sup>a</sup>, R. Stevens <sup>a</sup>, M. Cain <sup>b</sup>, M. Stewart <sup>b</sup>

<sup>a</sup> *Materials Research Centre, Department of Engineering & Applied Science, University of Bath, UK*

<sup>b</sup> *Materials Centre, National Physical Laboratory, Teddington, Middlesex, UK*

\* Corresponding author. Tel.: +44-1225-383062; fax: +44-1225-386098.  
*E-mail address: ea2aced@bath.ac.uk (A.C. Dent).*

## **Abstract**

The availability of fine scale PZT fibres has enabled advances in actuator and sensor applications, including devices for structural control such as the Active Fibre Composite (AFC). Since PZT fibres form active elements within a functional device, fibre characterisation and optimisation is essential. Several commercially available fibres have been studied, which are representative of the two dominant processing routes currently utilised: extrusion and suspension spinning. Fibres have been characterised in terms of morphology (shape factor and diameter variability), microstructure (grain size and porosity,) and phase composition (XRD). Certain fibres were found to exhibit properties unsuitable for AFC applications, which suggests that commercial production of fine scale PZT fibres may not yet be fully optimised.

*Keywords: B. Fibres; B. Microstructure-final; Morphology; D. PZT; B. X-ray methods.*

## 1. Introduction

Lead zirconate titanate (PZT) fibres present the engineer with an attractive form of active material, which is suitable for inclusion into composite structures and novel actuator and sensor devices. Availability of these materials has enabled the development of Active Fibre Composites (AFCs), comprised of uniaxially aligned piezoelectric fibres embedded in a polymer matrix, with interdigitated surface electrodes<sup>1</sup>. AFC devices have been investigated for novel applications including contour control, vibration suppression and structural health monitoring.

Processing and optimisation of piezoelectric fibres is an active research area, from which three principle manufacturing routes have emerged- extrusion<sup>2</sup>, sol-gel<sup>3</sup> and suspension spinning<sup>4,5</sup>. Current production methods differ primarily in the precursor materials, whether a mixed oxide powder (extrusion and suspension spinning), or wet chemical (sol-gel) route is selected. This may affect stoichiometric control, and the resulting properties of the PZT solid solution. Production methods also differ in the shaping of the green fibres. Fabrication can broadly be classified by whether the stock material is formed under compression (extrusion), or tension (sol-gel and suspension spinning). It is possible that these contrasting processing conditions will cause microstructural and morphological differences in the fibres, which may ultimately affect piezoelectric performance.

Studies of PZT fibres have predominantly focused on characterising the electromechanical coefficients of the material<sup>6</sup>, with few publications relating morphology and microstructure to processing history<sup>7</sup>. The aim of this paper is to present a comparative study of PZT fibres manufactured by different methods. Characterisation of fibre morphology, microstructure and phase composition will be related to the manufacturing processes and discussed with reference to AFC applications.

## **2. Experimental**

### *2.1 Materials*

PZT (5A) fibres were obtained for the Alceru, Extrusion, Viscose Suspension Spinning and Viscous Plastic Processing manufacturing methods (Table 1). Fibres were supplied by three commercial enterprises, with exception of the viscous plastic processed fibres that were produced at the Interdisciplinary Research Centre in Materials, University of Birmingham.

Extrusion is well suited to forming ceramic fibres, and as an established technology may prove the most commercially viable<sup>2</sup>. Viscous plastic processing (VPP) differs from conventional extrusion processes, in the use of higher viscosity ceramic-plastic dough than conventional extrusion pastes<sup>8</sup>. Suspension spinning methods have been adapted from textile processing techniques, where the ceramic loaded carrier material is

coagulated and burnt-out after spinning. Precursor materials utilised are viscose (VSSP)<sup>4</sup>, or cellulose with the Alceru (Alternative Cellulose Rudolstadt) method<sup>5</sup>.

## 2.2 Morphology

Macrostructural features are relevant to device manufacture, since active fibre composites require semi-continuous lengths of straight fibres, to achieve an even monolayer with controllable periodicity. Fibre cross section must be consistent along the fibre and between fibres, to ensure good contact between the electrode and active material layer and prevent electrical breakdown or poor strain response<sup>9</sup>.

Fibre morphology was characterised by image analysis of fibre cross sections to determine shape factors and diameter variability. Samples were prepared for each material with an excess of 100 unique fibres, which were vertically aligned in potting moulds and infiltrated with an epoxy resin. After curing, the samples were ground until planar, polished and gold sputtered before imaging by scanning electron microscopy (SEM, Jeol JSM-6310). Digital micrographs were recorded and image analysis software (ImageTool, UTHSCSA) used to identify and analyse fibres, to compute area ( $A$ ), and maximum ( $D_{max}$ ) and minimum ( $D_{min}$ ) calliper lengths. Results from 100 fibres per material were used to calculate feret diameter ( $D_A$ ), Elongation ( $SF_E$ ) and Compactness ( $SF_C$ ) shape factors. Elongation is dependent on the ratio of minimum to maximum calliper diameters (Eqn. 1), and Compactness describes the similarity of a measured feature to a circle (Eqn. 2).

$$SF_E = \frac{D_{\min}}{D_{\max}} \quad (1)$$

$$SF_C = \frac{\sqrt{(4 \times A/\pi)}}{D_{\max}} \quad (2)$$

Both indices have a value of one for a perfect circle and lower values reflect deviation from a uniform cross-section. It was found that an arbitrary ‘Uniformity’ shape factor, calculated from the product of Elongation and Compactness, provided a convenient parameter for fibre comparison. Reliable measurements of fibre diameter were achieved by assuming a circular cross section and calculating the feret, or area equivalent, diameter (Eqn. 3).

$$D_A = \sqrt{4A/\pi} \quad (3)$$

### 2.3 Microstructure

Microstructure was characterised for the different fibre materials by two key properties: grain structure and porosity. It is well documented that small grain sizes are detrimental to piezoelectric coupling due to the increased volume of grain boundary interfaces<sup>10</sup> and impediment of domain formation<sup>11</sup>. Well consolidated piezoceramics are required to develop good electromechanical coupling, thus high density and low porosity is desirable for actuator applications<sup>12</sup>.

The samples prepared for morphological study were etched (12.5ml HNO<sub>3</sub>, 2.5ml HF, 8.5ml H<sub>2</sub>O) to reveal the grain structure for SEM inspection. To ensure the grains perpendicular to the fibre length were representative of the bulk material, earlier microscopy of exterior grains and fracture surfaces had demonstrated equiaxed grains of comparable dimension. The samples were examined and digital micrographs recorded for five randomly selected fibres of each material. Grain size was measured by a linear intercept method due to the efficiency with which large areas can be surveyed. Although the average grain size determined by this technique is less than the true grain size, it is a useful comparative parameter. The linear intercept method was followed as described in BS623-3<sup>13</sup> using image analysis software, and ensuring that in excess of 500 grains were sampled for each material.

For each material 100 fibres were individually measured in length (typically 150±0.5mm), the mass determined on an analytical balance (±0.5mg) and the apparent bulk density found using the previously determined average fibre diameter to calculate volume. The percentage of the theoretical density of PZT 5A (7.75Mg/m<sup>3</sup>) was calculated to indicate porosity present, and numerical results were compared with SEM observations.

#### *2.4 Composition*

X-ray diffraction was used to identify the phases present and measure the relative proportion of these phases. The existence of both rhombohedral and tetragonal phases indicates a composition close to the morphotropic phase boundary, with enhanced

piezoelectric performance. The exact composition for optimum activity is difficult to predict, but it has been shown that the tetragonal-rhombohedral phase ratio strongly influences the piezoelectric constants of fibres, as in bulk PZT<sup>14</sup>.

Sintered fibres in the un-poled state were ground to a fine powder using a pestle and mortar. X-ray diffraction was performed with a Phillips powder diffractometer fitted with a 4kW x-ray generator, copper target and a graphite monochromator. Control of the diffractometer was achieved using the supplied diffraction software (PW1877 PC-APD Version 3.5b, Oct 1999). To assess the phases present a wide-angle scan was performed from two-theta of 20° to 60°, while a high-resolution scan was performed in the two-theta range 43° to 46° to quantify the phase proportions. Integral intensities were calculated for the de-convoluted reflection peaks associated with the tetragonal and rhombohedral phases, and the relative phase content calculated<sup>15</sup>.

### **3. Results and discussion**

#### *3.1 Morphology*

Processing history was found to influence fibre geometry, with irregularities visible in cross-sections for certain materials (Fig. 1). Low values for the Uniformity shape factor were noted for A125 and VSSP fibres, both produced via spinning processes (Table 2). The A125 fibres display a flattened edge as a consequence of creep deformation prior to sintering. Irregular cross-sections typical of the VSSP fibres may result from the

spinning technology used. Fibres produced by VPP exhibited high uniformity, with consistent circular cross-sections.

To assess variability of fibre diameter within each material sample, the coefficient of variability was calculated (Table 2). Lowest variability was found for the VPP material (1.7%), and the highest for VSSP fibres (5.1%). This supports the findings from shape factor analysis, suggesting that fibres prepared by viscose suspension spinning may cause an uneven monolayer with poor electrode contact when used for AFC production.

### *3.2 Microstructure*

Measured grain sizes varied considerably between the different materials (Table 3). Since the grains present in the VSSP material are significantly larger and more constant in size, it is probable that the stock material was formed from coarser grained powder (Fig. 2). Although it is expected that the larger grained fibres will exhibit greater piezoelectric activity, other factors may have a more dominant influence, specifically composition.

The materials investigated, with the possible exception of the extruded fibres, are sufficiently dense that reduction in piezoelectric performance will be small (Table 3). Fibres formed by the VPP process have notably high densities (99%), which may result from the high ceramic loading and extensive shear mixing process prior to fibre forming. The relatively low density of the extruded fibres (84%), may originate from problems with PZT loading, de-agglomeration or de-airing. During handling it was



observed that the extruded fibres were particularly fragile. This highlights the further importance of achieving a high density fibre, to ensure adequate strength and robustness required for AFC manufacture and operation.

### *3.3 Composition*

The XRD profiles for the five fibre types are presented in Fig. 3. All reflections can be accounted for using the PZT reference spectrum. This confirms the absence of any non-piezoelectric pyrochlore phase in the fibres. The results show all fibres possess a mixture of rhombohedral and tetragonal phases, thus their compositions lie close to the morphotropic phase boundary (MPB). Since both Alceru materials have an almost identical final composition, it can be inferred that they were formed from similar stock solutions and that good stoichiometric control was achieved during further processing. The extruded and VPP fibres have high percentages of the tetragonal phase, which occurs on the titanate rich side of the MPB. Compositions richer in the tetragonal phase have been shown to exhibit improved piezoelectric activity<sup>15</sup>. Therefore, it is expected that the VPP and extruded fibres should display favourable piezoelectric activity, while both Alceru fibres and the VSSP fibres should display similar, but reduced activity.

## **4. Conclusions**

It has been shown that processing methods influence fibre morphology, microstructure and composition, which are important parameters in fibre performance and ease of incorporation into novel composite devices. The observed uneven cross-sections, small

grain sizes and porosity for some of the fibres studied, suggest that current processing technology may not yet be optimised. Kornmann and Huber<sup>7</sup> have also reported similar findings for fibres produced by certain manufacturing methods.

From comparative study, it can be concluded that fibres produced by the VPP method exhibit good morphology, moderate grain size and excellent sintered density. Although the extruded fibres had reasonable morphology, the small grain size and high porosity would indicate poor piezoelectric performance. These results are consistent with detailed electromechanical characterisation of similar fibres, previously reported<sup>6</sup>.

### **Acknowledgements**

Fibres prepared by viscous plastic processing were kindly supplied by G. Dolman, B. Su & T. Button, IRC in Materials, University of Birmingham. The author is grateful for the financial support of the National Physical Laboratory and the EPSRC PRIME Faraday partnership.

## References

1. Bent, A. A. & Hagood, N. W., Piezoelectric fibre composites with interdigitated electrodes. *J. Int. Mat. Syst. Struct.*, 1997, **8**, 903-919.
2. Strock, H. B., Pascucci, M. R., Parish, M. V., Bent, A. A. & Shrout, T. R., Active PZT fibers, a commercial production process. *SPIE Conf. Proc.*, 1999, **3675**, 22-31.
3. Meyer, R. J., Shrout, T. R. & Yoshikawa, S., Lead zirconate titanate fine fibers derived from alkoxide-based sol-gel technology. *J. Am. Ceram. Soc.*, 1998, **81**, 861-868.
4. French, J. D. & Cass, R. B., Developing Innovative Ceramic Fibers. *Am. Ceram. Soc. Bull.*, 1998, **76**, 61-65.
5. Meister, F., Vorbach, D., Niemz, F., Schulze, T. & Taeger, E., Functional high-tech-cellulose materials by the ALCER(R) process. *Materialwiss. Werkst.*, 2003, **34**, 262-266.
6. Nelson, L. J., Bowen, C. R., Stevens, R., Cain, M. & Stewart, M., Modelling and measurement of piezoelectric fibres and interdigitated electrodes for the optimisation of piezofibre composites. *SPIE Conf. Proc.*, 2003, **5053**, 556-567.
7. Kornmann, X. & Huber, C., Microstructure and mechanical properties of PZT fibres. *J. Eur. Ceram. Soc.*, 2004, **24**, 1987-1991.
8. Pearce, D., Dolman, G., Meggs, C. & Button, T., Viscous processed versus conventional piezoelectric ceramics: experimental comparisons using real world devices. In *Ferroelectrics 2000 UK*, eds. N. Alford & E. Yeatman. IOM Communications, London, 2000, pp. 145-152.
9. Kornmann, X., Huber, C. and Elsener, H. R., Piezoelectric ceramic fibers for active fiber composites: a comparative study. *SPIE Conf. Proc.*, 2003, **5056**, 330-337.
10. Randall, C., Namchul, K., Kucera, J., Cao, W. & Shrout, T., Intrinsic and extrinsic size effects in fine-grained morphotropic-phase-boundary lead zirconate titanate ceramics. *J. Am. Ceram. Soc.*, 1998, **81**, 677-688.
11. Arlt, G., Review: Twinning in ferroelectric and ferroelastic ceramics: stress relief. *J. Mater. Sci.*, 1990, **25**, 2655-2666.
12. Roncari, E., Galassi, C., Craciun, F., Capianna, C. & Piancastelli, A., A microstructural study of porous piezoelectric ceramics. *J. Eur. Ceram. Soc.*, 2001, **21**, 409-417.
13. BS EN 623-3:2001: Advanced technical ceramics- monolithic ceramics- general and textural properties- part 3: Determination of grain size and size distribution (characterised by the linear intercept method).
14. Steinhausen, R., Hauke, T., Beige, H., Watzka, W., Lange, U., Sporn, D., Gebhardt, S. & Schönecker, A., Properties of fine scale piezoelectric PZT fibers with different Zr content. *J. Eur. Ceram. Soc.*, 2001, **21**, 1459-1462
15. Mishra, S., Pandey, D. & Singh, A., Effect of phase coexistence at morphotropic phase boundary on the properties of  $\text{Pb}(\text{Zr}_x\text{Ti}_{1-x})\text{O}_3$  ceramics. *Appl. Phys. Lett.*, 1996, **69**, 1707-1709.

## **Tables**

**Table 1.** Fine scale PZT5A fibres selected for investigation.

**Table 2.** Morphological properties. Mean feret diameter ( $D_A$ ) and coefficient of variability (C.V.) is reported. Uniformity shape factor is expressed in percent, with mean values reported ( $\pm 1$  standard deviation to indicate variability).

**Table 3.** Microstructural properties. Average grain size as determined by the linear intercept method. Mean density is reported with  $\pm$  max. error limits calculated by propagation of error. Porosity has been estimated from the percentage of theoretical density achieved.

## **Figures**

**Figure 1.** Secondary electron images of fibre cross-sections. (a) A125, (b) VSSP, (c) VPP. 200 $\mu$ m scale bar.

**Figure 2.** Secondary electron images for polished fibre surfaces used to determine grain size, with inset (top right) of grains inspected along fibre exterior. (a) A125, (b) A250, (c) E130, (d) VPP, (e) VSSP. 10 $\mu$ m scale bar.

**Figure 3.** XRD profiles for the five fibre types. Proportion of rhombohedral phase (%R) has been indicated for each material.

**Table 1.**

Designation	Production method	Diameter / $\mu\text{m}$
A125	Alceru	125
A250	Alceru	250
E130	Extruded	130
VSSP	Viscose Suspension Spinning Process	235
VPP	Viscous Plastic Process	250

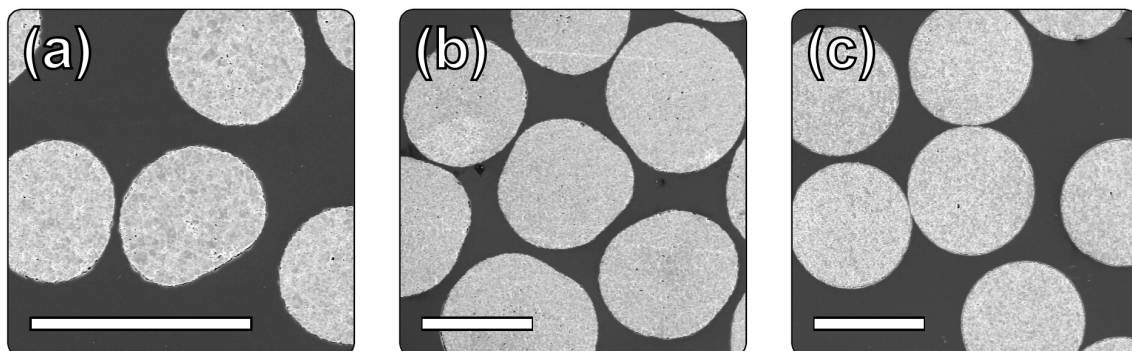
**Table 2.**

Material	Uniformity / %	$D_A$ / $\mu\text{m}$	C.V. $D_A$
A125	90 ( $\pm 6$ )	131	2.1 %
A250	96 ( $\pm 1$ )	263	2.4 %
E130	94 ( $\pm 2$ )	134	2.4 %
VSSP	90 ( $\pm 4$ )	251	5.1 %
VPP	96 ( $\pm 1$ )	233	1.7 %

**Table 3.**

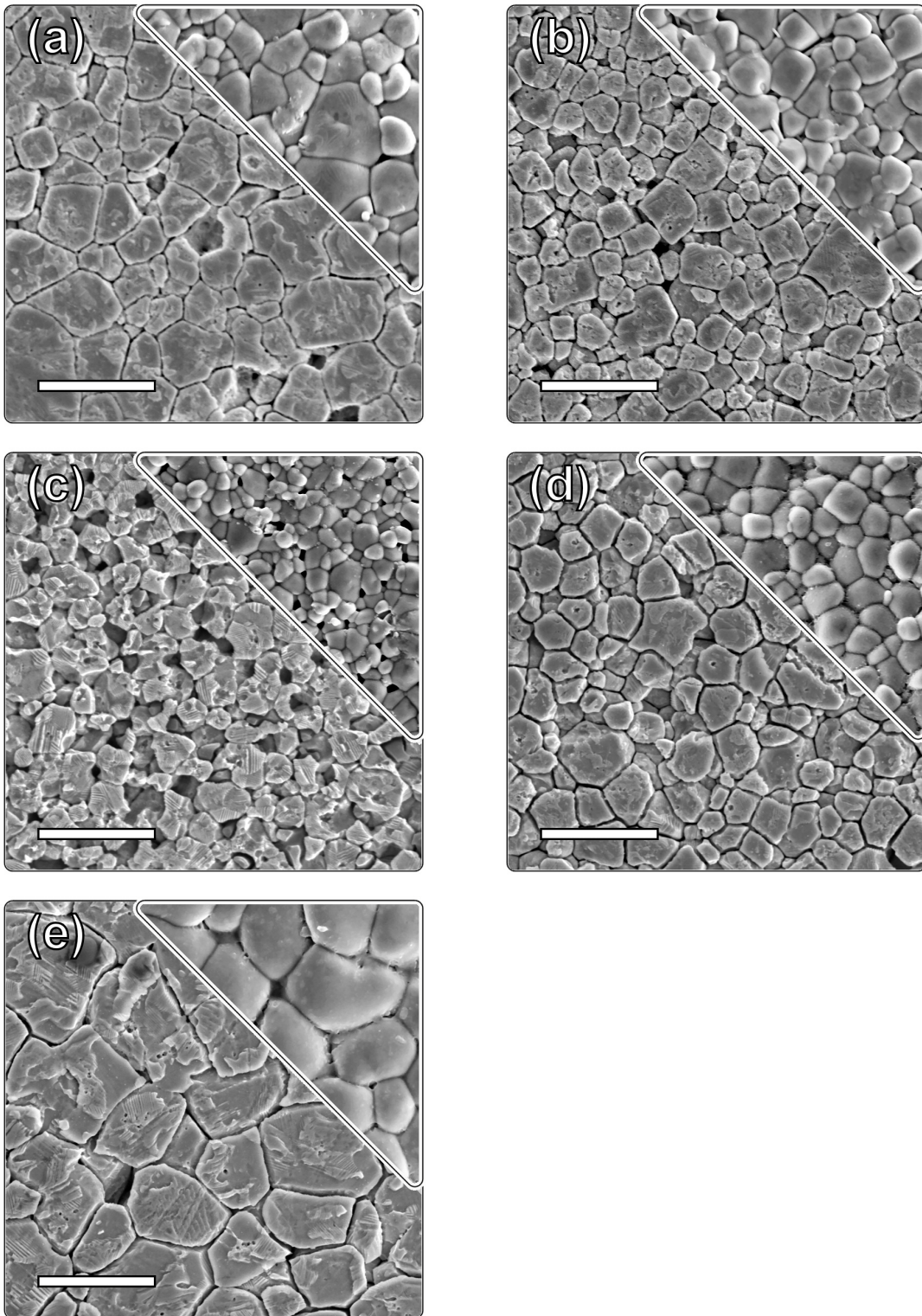
Material	Grain size / $\mu\text{m}$	Density / $\text{Mg m}^{-3}$	Porosity
A125	2.9	7.2 ( $\pm 0.3$ )	8 %
A250	2.0	7.4 ( $\pm 0.1$ )	4 %
E130	2.2	6.5 ( $\pm 0.5$ )	16 %
VSSP	5.9	7.5 ( $\pm 0.2$ )	3 %
VPP	2.5	7.7 ( $\pm 0.1$ )	1 %

**Figure 1.**



(Images: Fig1a.jpg, Fig1b.jpg, Fig1c.jpg)

**Figure 2.**



(Images: Fig2a.jpg, Fig2b.jpg, Fig2c.jpg, Fig2d.jpg, Fig2e.jpg)

**Figure 3.**

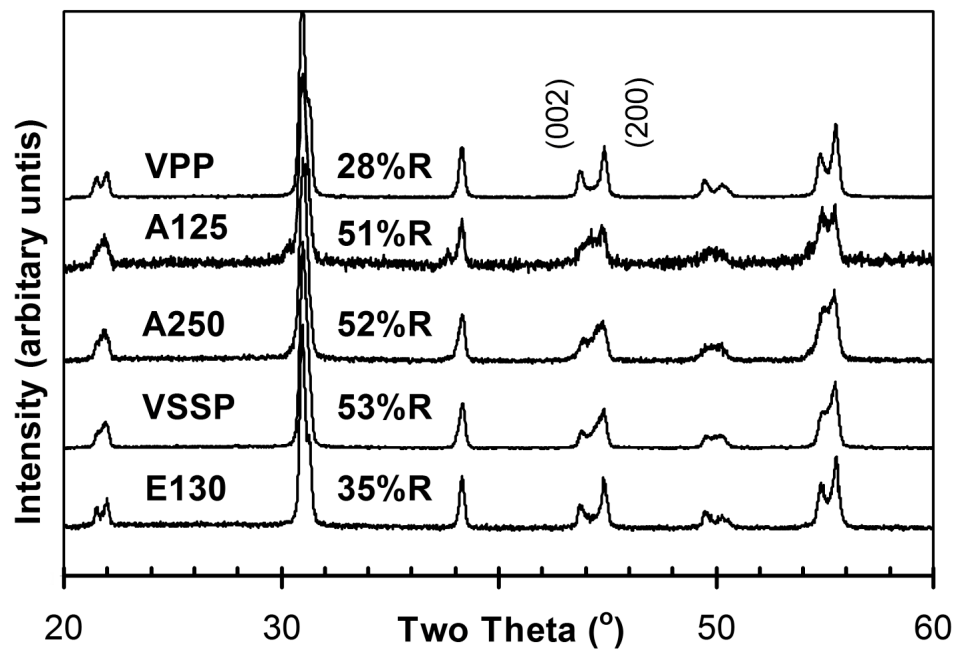


(Image: Fig3.tif)